XLIII CILAMCE
21–25, November, 2022
FOZ DO IGUAÇU – PR – BRAZIL

Study on the modeling of the actuation system of a quadrotor

Vitor Tucci Ramos[1], Reginaldo Cardoso[2], Décio C. Donha[2]

[1]*Lab. of Dynamics and Control (LDC), Dept. of Electrical Engineering, University of São Paulo (USP)*
Av. Prof. Mello Moraes, 2231, 05508-030, São Paulo-SP, Brazil
vitor.tucci@usp.br
[2]*Lab. of Dynamics and Control (LDC), Dept. of Mechanical Engineering, University of São Paulo (USP)*
Av. Prof. Mello Moraes, 2231, 05508-030, São Paulo-SP, Brazil
reginaldo.cardoso@usp.br, decdonha@usp.br

Abstract. This work compares the actuator model based on constants, the non-linear model of the actuator's components, and the experimental data. The actuation model is composed of the following components: electronic speed controller (ESC), motor and propeller. The non-linear modeling of the ESC will be done using the pulse width modulation signal (PWM) as input and the current as output. These current will be the input of the motor which will have as output the angular velocity which will be the input of the propeller model which will have as output thrust and torque. A helical trajectory was defined as a desired in the simulation. In both models, the integral backstepping control was applied. A comparison criterion was used the power consumption, which is one of the major barriers of these types of vehicles.

Keywords: Actuator Modelling, Integral Backstepping, Quadrotor

1 Introduction

The application of unmanned aerial vehicles (UAVs) has been increasing in recent years. This increase is due to its efficiency in carrying out certain activities, its adaptability to different missions and its relatively low cost [1]. According to [2], UAVs can be classified into two groups: fixed-wing vehicles and rotary-wing vehicles (which use rotors as lift). The rotary-wing vehicles, such as quadrotor, have high maneuverability and vertical take-off and landing (VTOL) [3]. Because of these advantages, these types of vehicles are more attractive than the fixed-wing [4]. However, rotary wing vehicles consume more energy, because they have a greater number of engines, limiting the flight time. A quadrotor, for example, has an autonomy of a few minutes of operation [1]. The main disadvantage of quadrotor is autonomy, which is limited by the capacity of the on-board battery. Many works in the control area are concerned only with obtaining the control law that generates the desired force or angular velocity in each actuator [3], [5]. Without considering that the control signal is a pulse-width modulation (PWM) type signal, which generates the desired power. Thus, this work focuses on the development of a control law for the input of the PWM signal.

2 Component Model

The quadcopters' propulsion system consists of four pairs of the motor-propeller assembly, an electronic speed controller (ESC). The motor used is a direct current brushless (DCB) type. The ESC is responsible for transforming a PWM signal into the motor input voltage. The rotation of the propeller is responsible for generating the thrust that will sustain the vehicle.

2.1 ESC Model

The control board sends PWM-type signals to the ESC, which in turn controls the voltage supplied to the motor and, consequently, its rotational speed. The PWM signal can be mapped to an 8-bit signal, represented by an integer between 0 and 255. The ESC loses a lot of energy in the form of heat, so for identification, the

input voltage U_{in}, the current I and the equivalent output voltage U_{out} are measured.We can approximate the data measured to a curve, which representing the ESC model, according to eq. (1) [6],

$$U_{out} = U_{in}\frac{PWM}{255}\left(\beta + \frac{\alpha}{I}\right) \tag{1}$$

where: $\alpha = 1.0692$ and $\beta = 0.5$.

2.2 DCB Motor Model

As it is a direct current motor and the current variation does not have a considerable frequency of oscillation, the effect of the inductance of the motor armature will be disregarded.

$$U_a = R_a I_a + K_e \omega \tag{2}$$

where: R_a is the armature resistance, U_a is the armature voltage, I_a the current, ω is the angular velocity of the motor and K_e is the electromotive force constant. The electromagnetic torque is given by

$$M = K_T I_a \tag{3}$$

where K_T is the electromotive torque constant. Combining the ESC output voltage with the motor armature voltage and assuming the armature current (U_a) is equal to the ESC current (U_{out}), then, isolating the current I

$$I = \beta\left(\frac{PWM}{255}U_{in}\right) + \sqrt{\left(\frac{PWM}{255}U_{in}\right)^2 + \alpha\frac{U_{in}}{R_a}} \tag{4}$$

where U_{in} is the battery voltage. The dynamic equation of the motor can be written as a combination of the eq. (2), eq. (3), and assuming that the load torque is identical to the propeller drag torque

$$\dot{\omega} = \frac{1}{J}\left[\frac{K_T U a}{R_a} - \omega\left(\frac{K_T K_e}{R_a}\right) - K_m\omega^2\right] \tag{5}$$

where K_m is a constant which depends of propeller.

2.3 Propeller Model

According to [6], a rotating propeller presents a thrust, which is a nonlinear quadratic equation

$$F = C_T\frac{4\rho R_h^4}{\pi^2}\omega^2 \quad \rightarrow \quad F = K_F\omega^2 \tag{6}$$

where ρ is the air density, R_h propeller radius, C_T the thrust coefficient, and ω the angular velocity. The propeller thrust coefficient is expressed as a function of the advance coefficient, which is the ratio of vehicle velocity to motor angular velocity [6]. It is possible to find the coefficient value on the propeller manufacturers' websites [7].

To calculate the power consumed in each of the actuators, we assume that the angular speed of each of the motors varies very little ($\dot{\omega} = 0$), which occurs with an almost constant thrust. We can calculate the voltage (U_a) from eq. (5), and the current (I_a) from eq. (2) at both equations the angular velocity is obtained from control law eq. (29), consequently, the power consumed, $P = I_a U_a$. Applying the results got, in eq. (4), it is possible to calculate the desired value of the PWM signal.

3 Approximation Actuator Model

According to [8] typical behavior of a propeller can be defined by two coefficients, thrust coefficient (C_T) used to calculated the propeller's thrust, like the eq. (6), and the power coefficient (C_P) which allow the calculated of the power's propeller.

$$P_P = C_P\frac{4\rho R_h^5}{\pi^3}\omega^3. \tag{7}$$

It can therefore also relate moment and thrust through the constant K_{TM}

$$M = \frac{C_P R_h}{C_T\pi}F \quad \rightarrow \quad M = K_{TM}F. \tag{8}$$

We can find the both coefficients at website of the manufactured, like [7]. In this case, the propeller chosen was 1245MR and the coefficients are $C_T = 0.0916$, $C_P = 0.0412$, and $K_{TM} = 0.0218m$. Another coefficient is the K_V, which characterizes how the angular velocity of a certain DC motor evolves with power supply voltage. This allows to know how many RPM the motor provide per each Volt. Then to obtained the consumed Volt of the motor angular velocity of the motor per Volt (U_a)

$$\omega = \frac{2\pi K_V}{60} U_a \quad \rightarrow \quad U_a = \frac{\omega 60}{2\pi K_V}. \tag{9}$$

To get the current consumption, it is necessary to assume that the thrust is almost constant, $\dot{\omega} = 0$, then,

$$I = \frac{U_a}{R_a} - K_e \omega \tag{10}$$

and the power consumed is $P = IU_a$.

4 Vehicle Modeling and Control.

4.1 Vehicle Model

The quadrotor's 6 DOF nonlinear dynamic equations are written based on the principle Newton-Euler [3], as follows

$$\begin{cases} \dot{\boldsymbol{p}} &= \boldsymbol{R}_t \boldsymbol{v} \\ \dot{\boldsymbol{\Theta}} &= \boldsymbol{R}_r \boldsymbol{\omega} \end{cases} \tag{11}$$

$$\begin{cases} \dot{\boldsymbol{v}} &= \dfrac{1}{m}\left(\boldsymbol{F}_f - \boldsymbol{F}_d + \begin{bmatrix} 0 & 0 & mg \end{bmatrix}^T\right) \\ \dot{\boldsymbol{\omega}} &= \boldsymbol{J}^{-1}\left[\boldsymbol{M}_m - \boldsymbol{M}_d - \boldsymbol{\omega} \times \boldsymbol{J}\boldsymbol{\omega}\right] \end{cases} \tag{12}$$

where $\boldsymbol{p} = \begin{bmatrix} x & y & z \end{bmatrix}^T$ is the position vector, $\boldsymbol{v} = \begin{bmatrix} u & v & w \end{bmatrix}^T$ is the linear velocity vector, $\boldsymbol{\Theta} = \begin{bmatrix} \phi & \theta & \psi \end{bmatrix}^T$ is the attitude vector, $\boldsymbol{\omega} = \begin{bmatrix} p & q & r \end{bmatrix}^T$ is the angular velocity vector, m is the vehicle mass, $\boldsymbol{J} = diag(I_{xx}, I_{yy}, I_{zz})$ is the inertia matrix. The matrices $\boldsymbol{R}_r$ and $\boldsymbol{R}_t$ are,

$$\boldsymbol{R}_r = \begin{bmatrix} 1 & S\psi t\theta & C\phi t\theta \\ 0 & C\theta & -S\theta \\ 0 & S\phi/S\theta & C\phi/S\theta \end{bmatrix}, \quad \boldsymbol{R}_t = \begin{bmatrix} C\theta C\psi & C\psi S\theta S\phi - S\psi C\phi & C\psi S\theta C\phi + S\psi S\phi \\ C\theta S\psi & S\psi S\theta S\phi + C\psi C\phi & S\psi S\theta C\phi - C\psi S\phi \\ -S\theta & S\phi C\theta & C\phi C\theta \end{bmatrix}.$$

$\boldsymbol{F}_f$ is the total thrust produced via the sum of the four propellers ($F_z = \sum_{i=1}^{4} F_i$) with respect to the navigation-fixed

$$\boldsymbol{F}_f = -\frac{1}{m} \begin{bmatrix} C\phi S\theta C\psi + S\phi S\psi \\ C\phi S\theta S\psi - S\phi C\psi \\ C\phi C\theta \end{bmatrix} F_z = \boldsymbol{M}_V F_z \tag{13}$$

where Cx, Sx and tx designated $\cos(x)$, $\sin(x)$, and $\tan(x)$ respectively. $\boldsymbol{F}_d = diag(fd_x, fd_y, fd_z)|\boldsymbol{v}|\boldsymbol{v}$, is the drag force, and fd_x, fd_y and fd_z are the drag coefficients. The term $\boldsymbol{M}_m = \begin{bmatrix} M_x & M_y & M_z \end{bmatrix}^T$ denotes the moment developed by four rotors of the vehicle. The term $\boldsymbol{M}_d = diag(md_\phi, md_\theta, md_\psi)|\boldsymbol{\omega}|\boldsymbol{\omega}$ is the drag torques with md_ϕ, md_θ and md_ψ are the drag coefficients.

Renaming variables as follows $\dot{\boldsymbol{x}}_1 = \boldsymbol{x}_2 = \begin{bmatrix} \dot{x} & \dot{y} & \dot{z} \end{bmatrix}^T$, and $\dot{\boldsymbol{x}}_3 = \boldsymbol{x}_4 = \begin{bmatrix} \dot{\phi} & \dot{\theta} & \dot{\psi} \end{bmatrix}^T$, consequently the complete dynamic model which governs the quadrotor is as follows

$$\begin{aligned} \dot{\boldsymbol{x}}_1 &= \boldsymbol{x}_2, \\ \dot{\boldsymbol{x}}_2 &= \boldsymbol{\Delta_f} + \boldsymbol{F}_f \end{aligned} \tag{14}$$

where: $\boldsymbol{\Delta f} = \dot{\boldsymbol{R}}_t \boldsymbol{\nu} + \boldsymbol{R}_t \left(-\boldsymbol{F}_d + \begin{bmatrix} 0 & 0 & mg \end{bmatrix}^T\right)$, and $\boldsymbol{v} = (\boldsymbol{R}_t)^{-1} \dot{\boldsymbol{x}}_1$.

$$\begin{aligned} \dot{\boldsymbol{x}}_3 &= \boldsymbol{x}_4, \\ \dot{\boldsymbol{x}}_4 &= \boldsymbol{\Delta_m} + \boldsymbol{B}\boldsymbol{M}_m, \end{aligned} \tag{15}$$

where: $\boldsymbol{\Delta m} = \dot{\boldsymbol{R}}_r\boldsymbol{\omega} + \boldsymbol{R}_r\left(-\boldsymbol{M}_d - \boldsymbol{\omega}\times\boldsymbol{J}\boldsymbol{\omega}\right)$, $\boldsymbol{B} = \boldsymbol{R}_r\boldsymbol{J}^{-1}$, and $\boldsymbol{\omega} = \left(\boldsymbol{R}_r\right)^{-1}\dot{\boldsymbol{x}}_3$.

4.2 Integral Backstepping Control

The control is divided in an attitude subsystem, responsible for controlling ϕ, θ, and ψ, and a position subsystem, responsible for controlling x, y, and z.

First step is to define a proportional-integrative position error ($\boldsymbol{z}_1$),

$$\boldsymbol{z}_1 = \boldsymbol{e}_1 + \boldsymbol{\beta}_1\int \boldsymbol{e}_1, \tag{16}$$

where $\boldsymbol{e}_1 = \boldsymbol{x}_1 - \boldsymbol{x}_{1d}$, with $\boldsymbol{x}_{1d}$ is the desired position vector, and $\boldsymbol{\beta}_1$ is a positive constant matrix. Defining a new variable ($\boldsymbol{z}_2$) that is dependent on the virtual control variable ($\boldsymbol{\alpha}_1$)

$$\boldsymbol{z}_2 = \boldsymbol{x}_2 - \boldsymbol{\alpha}_1. \tag{17}$$

Considering the velocity error $\boldsymbol{e}_2 = \boldsymbol{x}_2 - \boldsymbol{x}_{2d}$, with $\boldsymbol{x}_{2d}$ is the desired velocity vector. Isolating the variable $\boldsymbol{x}_2$ from eq. (17), and substituting it in the velocity error, we obtain $\boldsymbol{z}_2 = \boldsymbol{e}_2 + \boldsymbol{x}_{2d} - \boldsymbol{\alpha}_1$. The derivative of eq. (16) can be written as follows,

$$\dot{\boldsymbol{z}}_1 = \boldsymbol{z}_2 - \boldsymbol{x}_{2d} + \boldsymbol{\alpha}_1 + \boldsymbol{\beta}_1 e_1. \tag{18}$$

The next step is defined a *Lyapunov* function. The function was chosen same as the [9]

$$\boldsymbol{V}_1 = \boldsymbol{z}_1^T\frac{1}{2}\boldsymbol{z}_1. \tag{19}$$

Following the backstepping procedure, it is necessary to ensure that the derivative of the function *Lyapunov* is negatively defined

$$\dot{\boldsymbol{V}}_1 = \boldsymbol{z}_1^T(\boldsymbol{z}_2 - \boldsymbol{x}_{2d} + \boldsymbol{\alpha}_1 + \boldsymbol{\beta}_1\boldsymbol{e}_1), \tag{20}$$

the virtual control ($\boldsymbol{\alpha}_1$) is responsible for stabilizing $\boldsymbol{z}_1$ to zero,

$$\boldsymbol{\alpha}_1 = -\boldsymbol{K}_1\boldsymbol{z}_1 + \boldsymbol{x}_{2d} - \boldsymbol{\beta}_1\boldsymbol{e}_1, \tag{21}$$

where $\boldsymbol{K}_1$ is a positive diagonal matrix. The choice of $\boldsymbol{\alpha}$ was not able to guarantee the stabilization of $\boldsymbol{V}_1$

$$\dot{\boldsymbol{V}}_1 = -\boldsymbol{z}_1^T\boldsymbol{K}_1\boldsymbol{z}_1 - \boldsymbol{z}_1^T\boldsymbol{z}_2, \tag{22}$$

the first term of eq. (22) is negative semi-defined because this term is equal to zero in the origin ($\boldsymbol{z}_1 = 0$), on the other hand, the second term can not be determined, so this second term must be eliminated to ensure that eq. (22) become negative-defined.

Considering the second *Lyapunov* function $\boldsymbol{V}_2 = \boldsymbol{V}_1 + \boldsymbol{z}_2^T\frac{1}{2}\boldsymbol{z}_2$, and its derivative can be calculated

$$\dot{\boldsymbol{V}}_2 = -\boldsymbol{z}_1^T\boldsymbol{K}_1\boldsymbol{z}_1 - \boldsymbol{z}_1^T\boldsymbol{z}_2 + \boldsymbol{z}_2^T\left(\dot{\boldsymbol{x}}_2 - \dot{\boldsymbol{x}}_{2d} + \boldsymbol{K}_1\left(\boldsymbol{z}_2 - \boldsymbol{K}_1\boldsymbol{z}_1\right) + \boldsymbol{\beta}_1\left(\boldsymbol{z}_2 - \boldsymbol{K}_1\boldsymbol{z}_1 - \boldsymbol{\beta}_1\boldsymbol{e}_1\right)\right) \tag{23}$$

Replacing $\dot{\boldsymbol{x}}_2 = \boldsymbol{\Delta f}_2 + \boldsymbol{U}_{2b}$ in eq. (23),

$$\dot{\boldsymbol{V}}_2 = -\boldsymbol{z}_1^T\boldsymbol{K}_1\boldsymbol{z}_1 - \boldsymbol{z}_1^T\boldsymbol{z}_2 + \boldsymbol{z}_2^T\left(\boldsymbol{\Delta f}_2 + \boldsymbol{U}_{2b} - \dot{\boldsymbol{x}}_{2d} + \boldsymbol{K}_1\left(\boldsymbol{z}_2 - \boldsymbol{K}_1\boldsymbol{z}_1\right) + \boldsymbol{\beta}_1\left(\boldsymbol{z}_2 - \boldsymbol{K}_1\boldsymbol{z}_1 - \boldsymbol{\beta}_1\boldsymbol{e}_1\right)\right), \tag{24}$$

for $\dot{\boldsymbol{V}}_2 < 0$, $\boldsymbol{U}_{2b}$ is chosen, with $\boldsymbol{K}_2$ being a constant positive diagonal matrix

$$\boldsymbol{U}_{2b} = \begin{bmatrix} F_{vx} & F_{vy} & F_{vz}\end{bmatrix}^T = -\boldsymbol{\Delta f}_2 + \dot{\boldsymbol{x}}_{2d} - \boldsymbol{K}_1\left(\boldsymbol{z}_2 - \boldsymbol{K}_1\boldsymbol{z}_1\right) + \boldsymbol{z}_1 - \boldsymbol{K}_2\boldsymbol{z}_2 - \boldsymbol{\beta}_1\left(\boldsymbol{z}_2 - \boldsymbol{K}_1\boldsymbol{z}_1 - \boldsymbol{\beta}_1\boldsymbol{e}_1\right). \tag{25}$$

Therefore, applying eq. (25) in eq. (24), we get that

$$\dot{\boldsymbol{V}}_2 = -\boldsymbol{z}_1^T\boldsymbol{K}_1\boldsymbol{z}_1 - \boldsymbol{z}_2^T\boldsymbol{K}_2\boldsymbol{z}_2 \tag{26}$$

the $\dot{\boldsymbol{V}}_2$ is a negative semi-defined function, which is enough to ensure the stability of the system. According to [5], the desired *Euler* angles (ϕ_d, θ_d) and F_z, for the vehicle to follow the desired trajectory, these can be obtained from eq. (13)

$$F_z = \boldsymbol{M}_V^T\left(\boldsymbol{M}_V\boldsymbol{M}_V^T\right)^{-1}\boldsymbol{F}_f$$

$$\phi_d = \arcsin\left(m\frac{F_{vx}\cos(\psi) - F_{vy}\sin(\psi)}{F_{vz}}\right), \qquad \theta_d = \arctan\left(\frac{-F_{vx}\sin(\psi) + F_{vy}\cos(\psi)}{F_z}\right). \tag{27}$$

The same approach was used for the attitude control. The ending expression ($\boldsymbol{U}_{4b}$) of the control input can be written

$$\boldsymbol{U}_{4b} = -\boldsymbol{\Delta f}_4 + \dot{\boldsymbol{x}}_{4d} - \boldsymbol{K}_3\left(\boldsymbol{z}_4 - \boldsymbol{K}_3\boldsymbol{z}_3\right) + \boldsymbol{z}_3 - \boldsymbol{K}_4\boldsymbol{z}_4 - \boldsymbol{\beta}_3\left(\boldsymbol{z}_4 - \boldsymbol{K}_3\boldsymbol{z}_3 - \boldsymbol{\beta}_3\boldsymbol{e}_3\right) \tag{28}$$

where $\boldsymbol{K}_3$, $\boldsymbol{K}_4$, and $\boldsymbol{\beta}_3$ are positive constant matrix, and $\boldsymbol{e}_3 = \boldsymbol{x}_3 - \boldsymbol{x}_{3d}$ the attitude error with $\boldsymbol{x}_{3d}$ the desired attitude,

$$\boldsymbol{z}_3 = \boldsymbol{e}_3 + \boldsymbol{\beta}_3\int \boldsymbol{e}_3 \qquad \boldsymbol{\alpha}_3 = -\boldsymbol{K}_3\boldsymbol{z}_3 + \boldsymbol{x}_{4d} - \boldsymbol{\beta}_3\boldsymbol{e}_3$$
$$\boldsymbol{e}_4 = \dot{\boldsymbol{e}}_3 = \boldsymbol{x}_4 - \boldsymbol{x}_{4d} \qquad \boldsymbol{z}_4 = \boldsymbol{x}_4 - \boldsymbol{\alpha}_3$$

After obtaining the thrust and the desired torque, the next step is determined the angular velocity of each motor

$$\boldsymbol{\omega}^2 = \begin{bmatrix} -K_T & -K_T & -K_T & -K_T \\ 0 & -l_mK_T & 0 & l_mK_T \\ l_mK_T & 0 & -l_mK_T & 0 \\ -K_TK_{TM} & K_TK_{TM} & -K_TK_{TM} & K_TK_{TM} \end{bmatrix}^{-1} \begin{bmatrix} F_z \\ \boldsymbol{U}_{4b} \end{bmatrix}. \tag{29}$$

5 Simulation.

The desired trajectory was chosen that does not lead the actuators to saturation. A helical type signal was chosen, with a radius equal to 1m and a rise of 0.05m per second. No initial condition error on the trajectory. First, a simulation of the vehicle and the control was carried out. After obtaining the control effort, the desired angular velocity was calculated and, finally, the power consumed in each case was obtained.

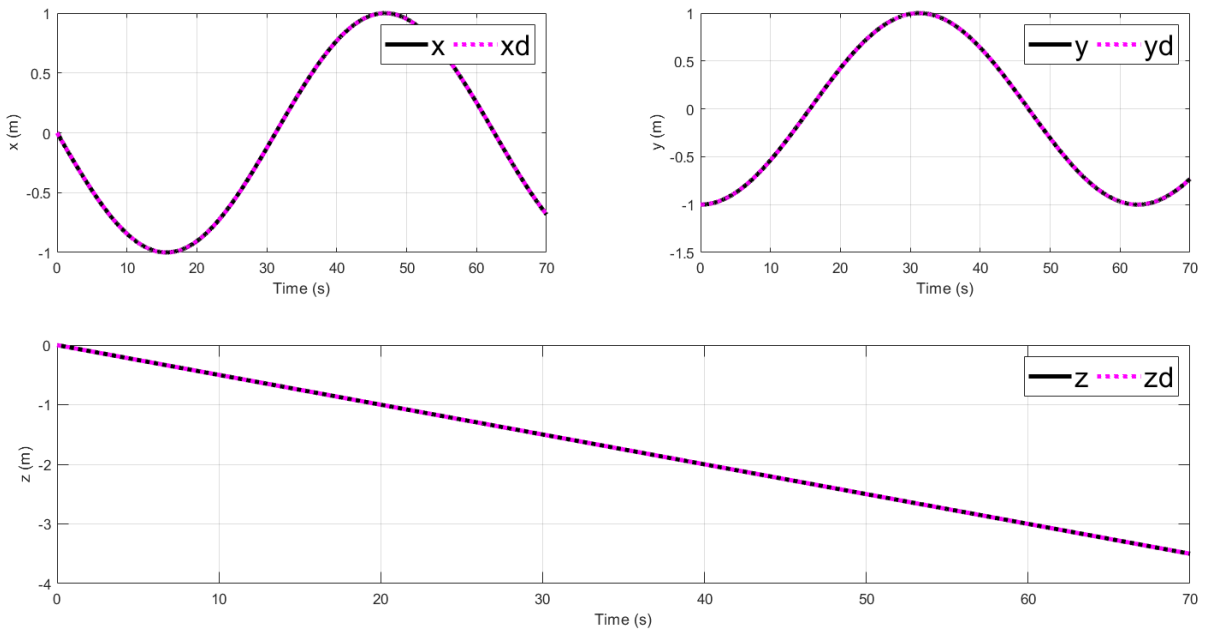

Figure 1. Helical movement of the vehicle along the x, y, z-axis. Curve in magenta desired trajectory and curve in black vehicle simulation.

Figure 1 shows the control result for a helical trajectory. It can be seen that the vehicle tracking the desired trajectory without position error.

Figure 2 shows the comportment of the vehicle's attitude towards a helical trajectory. It can be seen that the initial instants of the simulation, in all three graphics, have an oscillation. This occurs because the angle has to decompose the vertical force, to start the tracking the desired trajectory.

Figure 3 shows the angular velocity necessary, in each motor, to reach the desired trajectory. It can be seen that the initial instants of the simulation, all four graphics, have an oscillation. This occurs because of the angles' oscillation presented in the Fig. 2.

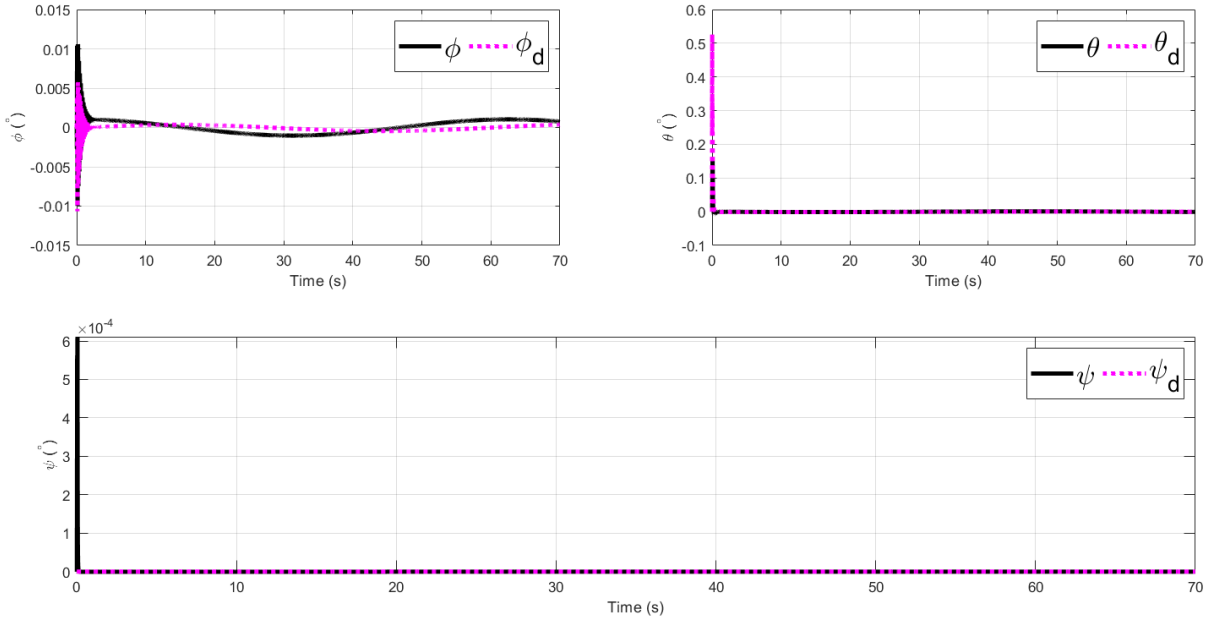

Figure 2. Comportment of the vehicle's attitude to a desired helical movement. Curve in magenta desired trajectory and curve in black vehicle simulation.

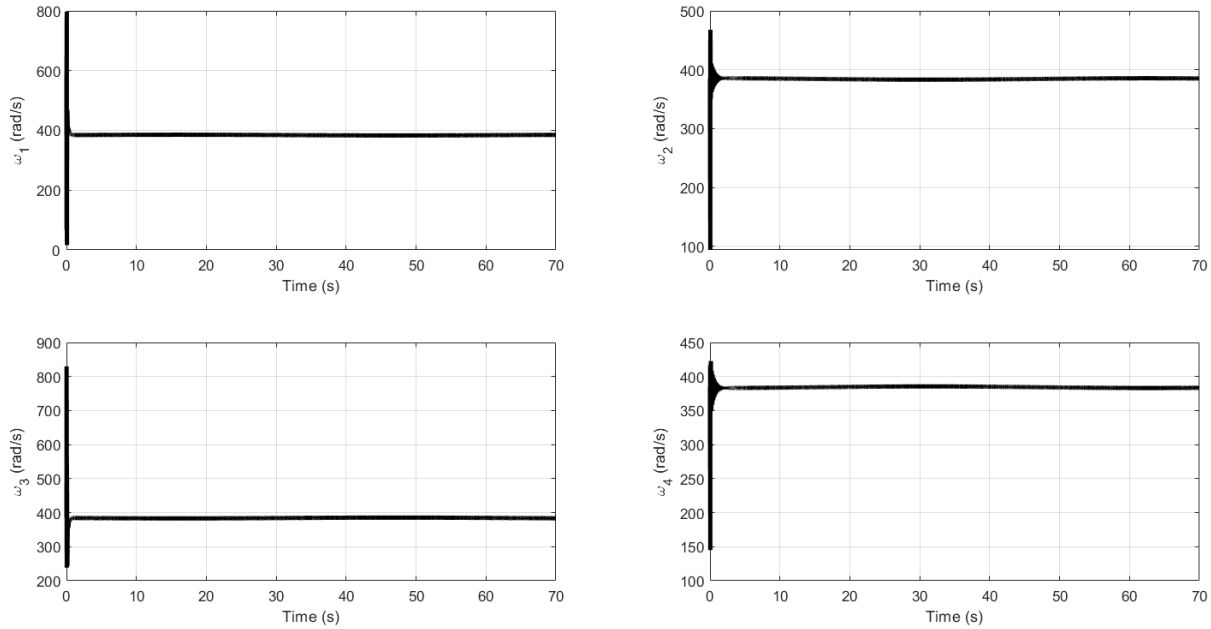

Figure 3. The angular velocity, in each motor, to vehicle tracking the desired trajectory, got from eq. (29)

Figure 4 shows the power consumed instantaneously, and the accumulated necessary for vehicle tracking the desired trajectory. It can be seen that the accumulated power of the model has an error equal to 2.28% and the model based on constant has an error equal to 19.67% compared with the experimental.

6 Conclusion.

The paper presents an actuator model, considering the ESC, motor and the propeller. Experimental tests to obtain the actuator model. This model was simulated with the integral backstepping control and calculated the power consumed. The power obtained was compared with a simple model based on constants provided by the data-sheets. It is possible to observe that the model got the power consumed almost equal with the experimental results. The error can be explained by some approximation during the experimental test. The division of the controller into position and attitude showed be able to control the generalized coordinates. Due to lack of space and by not adding

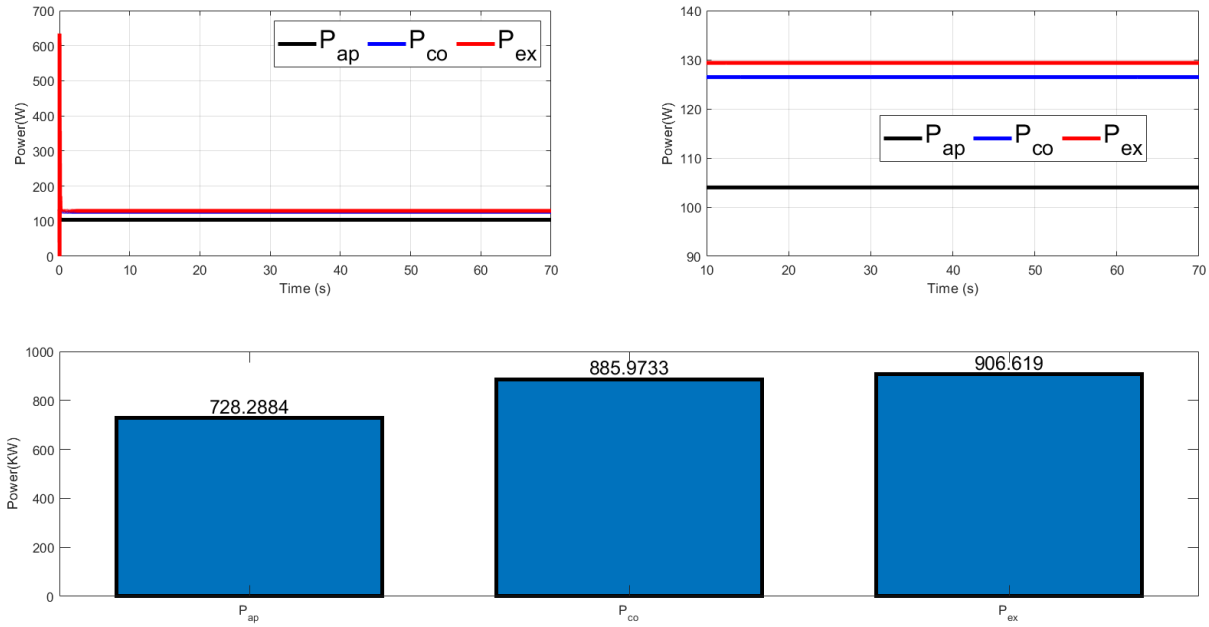

Figure 4. The power consumed in each modelling. Curve in red represents the experimental results (P_{ex}), curve in blue the components modelled (P_{co}), and curve in black approximation with the constants (P_{ap}). The bar graphic represents the power consumed by the vehicle in the desired trajectory.

any extra conclusions, the PWM signal were not presented. In addition, during all the simulations, the PWM signal did not reach saturation.

Acknowledgements. The second author acknowledge CAPES for the Ph.D. scholarships.

Authorship statement. The authors hereby confirm that they are the sole liable persons responsible for the authorship of this work, and that all material that has been herein included as part of the present paper is either the property (and authorship) of the authors, or has the permission of the owners to be included here.

References

[1] M. N. Boukoberine, Z. Zhou, and M. Benbouzid. A critical review on unmanned aerial vehicles power supply and energy management: Solutions, strategies, and prospects. *Applied Energy*, vol. 255, pp. 113823, 2019.
[2] A. Nourmohammadi, M. Jafari, and T. O. Zander. A survey on unmanned aerial vehicle remote control using brain-computer interface. *IEEE Transactions on Human-Machine Systems*, vol. 48, n. 4, pp. 337–348, 2018.
[3] A. C. F. Oliveira, J. A. T. Altuna, and D. P. F. Correa. Dynamic Modelling And Control Of Unmanned Aerial Vehicle Of The Quadrotor Type. In *Proceedings of the 25th International Congress of Mechanical Engineering*. ABCM, 2019.
[4] N. Wang, S. F. Su, M. Han, and W. H. Chen. Backpropagating Constraints-Based Trajectory Tracking Control of a Quadrotor with Constrained Actuator Dynamics and Complex Unknowns. *IEEE Transactions on Systems, Man, and Cybernetics: Systems*, vol. 49, n. 7, pp. 1322–1337, 2019.
[5] Y. Qi, J. Jiang, J. Wu, J. Wang, C. Wang, and J. Shan. Autonomous landing solution of low-cost quadrotor on a moving platform. *Robotics and Autonomous Systems*, vol. 119, pp. 64–76, 2019.
[6] A. Sendobry. *Control System Theoretic Approach to Model Based Navigation*. Phd thesis, Technische Universität Darmstadt:, 2013.
[7] APC Propellers. Propeller technical data, 2020.
[8] J. Miguel and B. Domingues. Quadrotor prototype. Master's degree in mechanical engineering, Technical University of Lisbon., 2009.
[9] R. Cardoso, M. E. M. Meza, E. Rafikova, and S. L. M. C. Titotto. Backstepping and integrative sliding mode control for trajectory tracking of a hybrid remotely operated vehicle. In *2017 IEEE International Conference on Robotics and Biomimetics (ROBIO)*, pp. 116–121, 2017.